Distributed Differential Space-Time Spreading for the Asynchronous Relay Aided Interference-Free Cooperative CDMA Uplink

S. Sugiura[1,2] **S. Chen**[1] **and L. Hanzo**[1]
[1]School of ECS, University of Southampton, SO17 1BJ, UK, Tel: +44-23-8059-3125, Fax: +44-23-8059-4508
Email: {ss07r,sqc,lh}@ecs.soton.ac.uk, http://www-mobile.ecs.soton.ac.uk
[2]TOYOTA Central R&D Labs., Inc., Aichi, 480-1192, Japan, Tel: +81-561-71-7163, Fax: +81-561-63-5258
Email: sugiura@mosk.tytlabs.co.jp, http://www.tytlabs.co.jp/eindex.html

***Abstract*—In this paper, we propose a differential Space-Time Coding (STC) scheme designed for asynchronous cooperative networks, where neither channel estimation nor symbol-level synchronization is required at the cooperating nodes. More specifically, our system employs differential encoding during the broadcast phase and a Space-Time Spreading (STS)-based amplify-and-forward scheme during the cooperative phase in conjunction with interference rejection Direct Sequence (DS) spreading codes, namely Loosely Synchronized (LS) codes. The LS codes exhibit a so-called Interference Free Window (IFW), where both the auto-correlation and cross-correlation values of the codes become zero. The IFW allows us to eliminate both the Multi-User Interference (MUI) as well as the potential dispersion-induced orthogonality degradation of the cooperative space-time codeword and the interference imposed by the asynchronous transmissions of the relay nodes. Furthermore, the destination node can beneficially combine both the directly transmitted and the relayed symbols using low-complexity correlation operations combined with a hard-decision detector. Our simulation results demonstrate that the proposed Cooperative Differential STS (CDSTS) scheme is capable of combating the effects of asynchronous uplink transmissions without any Channel State Information (CSI), provided that the maximum synchronization delay of the relay nodes is within the width of IFW. It will be demonstrated that in the frequency-selective environment considered our CDSTS arrangement is capable of exploiting both space-time diversity and multi-path diversity with the aid of a RAKE combiner.**

I. Introduction

Multiple-antenna-element assisted tranceiver design allows us to eliminate some of the limitations potentially preventing reliable wireless communications. For example, the family of Space-Time Codes (STCs) constitute efficient diversity techniques that are capable of combating the time-varying fading effects of wireless channels. Motivated by the concept of STCs, Space-Time Spreading (STS) [1] was also proposed, in order to achieve a transmit diversity gain with the aid of spreading the transmitted signals across multiple antennas in the context of Direct-Sequence Code Division Multiple Access (DS-CDMA) systems [2]. However, the antenna elements of colocated Multiple-Input Multiple-Output (MIMO) systems typically suffer from spatially correlated large-scale fading imposed by the shadowing effects. In order to eliminate this correlation-induced diversity-gain erosion, cooperative STC schemes [3], [4] were proposed to achieve the best attainable diversity gain of uncorrelated elements, where a collection of single-antenna-aided nodes act as a Virtual Antenna Array (VAA), having widely separated distributed antenna elements. On the other hand, attaining a high cooperative space-time diversity gain in a practical relay-aided network imposes further challenges. Firstly, many of the previously-proposed cooperative STC schemes assumed that perfect Channel State Information (CSI) of the Source-Relay (SR) links and/or of the Relay-Destination (RD) links is available at the destination receiver. However, the rapidly changing topology of vehicles travelling at high speeds makes it challenging to acquire accurate CSI, which results in a severe degradation of the achievable performance. Since each of the MIMO subchannels has to be sampled above the Doppler frequency, at high speeds an increased pilot overhead has to be tolerated for the sake of accurately estimating each MIMO channel component, which also gives rise to a substantial increase of the complexity. By contrast, inspired by the differential STC philosophy developed for collocated MIMO systems [5], a number of Cooperative Differential STCs (CDSTCs) were proposed in [6] in order to achieve reliable symbol detection without any CSI.

Another major challenge is the asynchronous nature of relay nodes in the network. The aforementioned cooperative STCs are all based on the assumption of perfect timing synchronization between the relay nodes, although in practice it is difficult to acquire accurate symbol-level time synchronization without imposing a high additional synchronization overhead and implementation complexity. As noted in [7], the resultant time synchronization errors impose a significant performance degradation. Additionally, the propagation delays arising both from the different node locations and from the multipath-induced delay-spread also contribute to the sampling offset errors, which further aggravates the effect of synchronization errors. To this end, a number of asynchronous cooperative STCs were proposed [8], [9], which invoke space-time equalization or multi-carrier transmission techniques, assuming that the perfect CSI and/or the relative transmission delays of the mobiles are available at the destination. However, a relatively high computational complexity is imposed at the destination receiver.

From a practical point of view, it is important to combat both the problems associated with the CSI estimation errors and the time synchronization errors, in order to achieve a useful cooperative space-time diversity gain. However, to the best of our knowledge, no differential STC schemes have been proposed for asynchronous cooperative scenarios. *Against this background, the main contribution of this paper is that we first propose a practical CDSTC scheme designed for asynchronous relay networks, where neither channel estimation nor symbol-level synchronization is required at any of the nodes. More specifically, our system employs differential encoding during the broadcast phase and an STS-based amplify-and-forward scheme during the cooperative phase in conjunction with interference rejection spreading codes, namely Loosely Synchronized (LS) spreading codes [10]. The LS codes exhibit a so-called Interference Free Window (IFW), where both the auto-correlation and cross-correlation values of the codes become zero, and hence have the capability of eliminating the Multi-User Interferences (MUIs) as well as the orthogonality degradation of the cooperative STC, which are imposed by the asynchronous nature of the relay nodes.*

II. System Overview

Consider a collection of $N_{\rm total} = M \times N$ nodes, each having a single antenna element and communicating with each other or with a specific destination node via frequency-flat fading channels, which corresponds to an uplink (UL) scenario or that of an ad

The financial support of the EU under the auspices of the Optimix project and of the EPSRC UK is gratefully acknowledged.

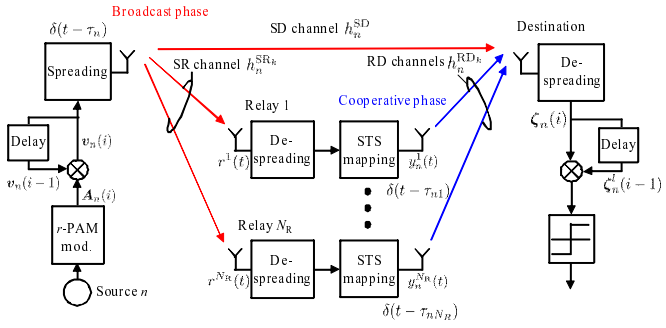

Fig. 1. Dual-phase transmission model of our CDSTS.

hoc network. We assume the employment of a Time Division aided CDMA (TD-CDMA) based channel allocation scheme, where a single TD transmission frame is divided into M time slots, where N DS-CDMA source nodes are supported in each of the M time slots with the aid of N unique, user-specific DS-CDMA spreading codes. More specifically, each transmission of the N source nodes is assisted by the preassigned source-specific N_{R} relay nodes, and the signal transmission involves two phases, i.e. the broadcast phase and the cooperative phase, assuming that the system is operated in a half-duplex mode. Additionally, in order to quantify the effects of asynchronously transmitting nodes on our CDSTS system, we introduce node-specific delays caused by their time synchronization errors, where the delays of the nth source node and that of the associated kth relay node are represented by τ_n and τ_{nk}, respectively. Furthermore, the Channel Impulse Responses (CIRs) of the source-relay channels, the source-destination channel and the relay-destination channels are described by $h_n^{\mathrm{SR}_k}\exp(j\theta_{nk}^{\mathrm{SR}})$, $h_n^{\mathrm{SD}}\exp(j\theta_n^{\mathrm{SD}})$ and $h_n^{\mathrm{RD}_k}\exp(j\theta_{nk}^{\mathrm{RD}})$, respectively, where $h_n^{\mathrm{SR}_k}$, h_n^{SD} and $h_n^{\mathrm{RD}_k}$ are the corresponding fading envelopes, while $\theta_{nk}^{\mathrm{SR}}$, θ_n^{SD} and $\theta_{nk}^{\mathrm{RD}}$ are the uniformly distributed phase-shift components.

Without loss of generality, we focus our attention on the first time slot, where each of the N sources communicates with a certain destination node with the aid of the N_{R} source-specific cooperating nodes selected from all the nodes, as illustrated in Fig. 1. To be specific, we consider the case of $N_{\mathrm{R}}=4$ relay nodes, where the resultant maximum space-time diversity order provided by the relay nodes is also four. Note that a single node may simultaneously act as the relay supporting different source nodes.

A. Transmitted Signal

During the broadcast phase of Fig. 1, each of the N source nodes transmits the differentially-encoded symbols both to the $N_{\mathrm{R}}=4$ relay nodes and to the destination node. Let the nth source node be the source-of-interest in this system model. First, the source bits $b_n(q)$ are mapped to r-bit PAM-modulated symbols and then the modulated symbols are Serial-to-Parallel (S/P) converted to the symbol blocks $\boldsymbol{a}_n(i)$, each containing four modulated symbols formulated as $\boldsymbol{a}_n(i)=[a_n^1(i)\ a_n^2(i)\ a_n^3(i)\ a_n^4(i)]^T$, where q and i represent the symbol and the block indices, respectively. Then, based on the symbol blocks $\boldsymbol{a}_n(i)$, the corresponding differentially-encoded symbol blocks $\boldsymbol{v}_n(i)=[v_n^1(i)\ v_n^2(i)\ v_n^3(i)\ v_n^4(i)]^T$ are generated as follows [11]: $\boldsymbol{v}_n(i)=\boldsymbol{A}_n(i)\boldsymbol{v}_n(i-1)/||\boldsymbol{v}_n(i-1)||$ with

$$\boldsymbol{A}_n(i)=\begin{bmatrix} a_n^1(i) & a_n^2(i) & a_n^3(i) & a_n^4(i) \\ -a_n^2(i) & a_n^1(i) & a_n^4(i) & -a_n^3(i) \\ -a_n^3(i) & -a_n^4(i) & a_n^1(i) & a_n^2(i) \\ -a_n^4(i) & a_n^3(i) & -a_n^2(i) & a_n^1(i) \end{bmatrix}, \quad (1)$$

where the first block $\boldsymbol{v}_n(0)=[1\ 1\ 1\ 1]^T$ is transmitted as a reference of the next differentially-encoded block, hence the first one does not containing any useful information. To relate the block index i to the symbol index q, let us define the qth differentially-modulated symbol as $\bar{v}_n(q)$, having the relation of $\bar{v}_n(4i+k-1)=v_n^k(i)$. Furthermore, the time-domain waveform transmitted by the nth source can be written as $s_n(t)=\sum_{q=-\infty}^{\infty}\bar{v}_n(q)\psi_{T_s^{\mathrm{S}}}(t-qT_s^{\mathrm{S}})$, where $\psi_\alpha(t)$ is the rectangular waveform, which is defined over the interval $[0,\alpha)$ and T_s^{S} represents the symbol duration of the broadcast phase.

Next, the differentially-modulated symbols $\bar{v}_n(t)$ are spread with the aid of the source's node-specific spreading code $c_n(t)=\sum_{i=0}^{L_{\mathrm{S}}-1}c_{ni}\psi_{T_c}(t-iT_c)$, where L_{S} is the code length of the spreading code and T_c is the chip duration, while c_{ni} represents the ith chip value. Here, we have the relation of $T_s^{\mathrm{S}}=L_{\mathrm{S}}T_c$. Note that the spreading factor G_{S} of the spreading code is given by the number of non-zero chips.

Having obtained the transmitted time-domain waveform $y_n(t)$ as $y_n(t)=\sqrt{\frac{P_{\mathrm{S}}}{G_{\mathrm{S}}}}\sum_{q=0}^{\infty}s_n(t)c_n(t-qT_s^{\mathrm{S}})$, the corresponding symbols received at the kth relay $r^k(t)$ and at the destination $r^{\mathrm{SD}}(t)$ are written as:

$$r^k(t)=\sum_{n=1}^{N}h_n^{\mathrm{SR}_k}y_n(t-\tau_n)\exp\left\{j(2\pi f_c t+\phi_n^{\mathrm{SR}_k})\right\}+n_k(t) \quad (2)$$

$$r^{\mathrm{SD}}(t)=\sum_{n=1}^{N}h_n^{\mathrm{SD}}y_n(t-\tau_n)\exp\left\{j(2\pi f_c t+\phi_n^{\mathrm{SD}})\right\}+n_{\mathrm{SD}}(t), \quad (3)$$

where we have $\phi_n^{\mathrm{SR}_k}=\theta_n^{\mathrm{SR}_k}-2\pi f_c\tau_n$ and $\phi_n^{\mathrm{SD}}=\theta_n^{\mathrm{SD}}-2\pi f_c\tau_n$, each given by the uniformly distributed random phase, while f_c is the operating carrier frequency. The noise components $n_k(t)$ of the kth relay and of the destination, namely $n_{\mathrm{SD}}(t)$ has a zero mean and variances of N_{0k} and $N_{0\mathrm{D}}$. Furthermore, P_{S} represents the transmission power of the source node, while $P_{\mathrm{R}}/4=(1-P_{\mathrm{S}})/4$ is that of each relay node, where the total transmission power is considered to be unity. It should be noted here that the Eqs. (2) and (3) take into account the effects of the asynchronous relationship between the source nodes by introducing the delay terms τ_n.

B. Relayed Signal

During the cooperative phase of Fig. 1, the $N_{\mathrm{R}}=4$ relay nodes *amplify-and-forward* the received signals to the destination node with the aid of the STS scheme. More specifically, each relay node constructs the STS codeword based on the preassigned four spreading codes $c_n^l(t)$ $(l=1,2,3,4)$, corresponding to the nth source, which are expressed as $c_n^l(t)=\sum_{i=0}^{L_{\mathrm{R}}-1}c_{ni}^l\psi_{T_c}(t-iT_c)$, where L_{R} is the code length of the spreading code and the symbol duration of the cooperating phase $T_s^{\mathrm{R}}=L_{\mathrm{R}}T_c$. Let us furthermore define the spreading factor of the codes $c_n^l(t)$ as G_{R}.

First, the kth relay node despreads the received signal $r^k(t)$ with the aid of the classic correlation operation using the spreading code $c_n(t)$, in order to obtain the despread symbol $\bar{d}_n^{\mathrm{SR}_k}(q)$ corresponding to the transmitted symbols $\bar{v}_n(q)$, which is given by

$$\bar{d}_n^{\mathrm{SR}_k}(q)=\sqrt{P_{\mathrm{S}}}h_n^{\mathrm{SR}_k}\bar{v}_n(q)+J_n^{\mathrm{SR}_k}(q)+N_n^{\mathrm{SR}_k}(q), \quad (4)$$

where $J_n^{\mathrm{SR}_k}(q)$ is the MUI-related term induced by the other source nodes' signals, which is given by

$$J_n^{\mathrm{SR}_k}(q)=\frac{1}{T_c}\sum_{n'\neq n}\sum_{q=0}^{\infty}\frac{\sqrt{P_{\mathrm{S}}}}{G_{\mathrm{S}}}h_{n'}^{\mathrm{SR}_k}\exp\left\{j(\phi_{n'}^{\mathrm{SR}_k}-\phi_n^{\mathrm{SR}_k})\right\} \times\int_{qT_s^{\mathrm{S}}+\tau_n}^{(q+1)T_s^{\mathrm{S}}+\tau_n}s_{n'}(t-\tau_{n'})c_{n'}(t-qT_s-\tau_{n'})c_n(t-\tau_n)dt \quad (5)$$

and $N_n^{\mathrm{SR}_k}(q)$ is the AWGN-related term formulated as

$$N_n^{\mathrm{SR}_k}(q)=\frac{1}{T_c\sqrt{G_{\mathrm{S}}}}\int_{qT_s^{\mathrm{S}}+\tau_n}^{(q+1)T_s^{\mathrm{S}}+\tau_n}n_k(t)c_n(t-\tau_n)e^{-j(2\pi f_c t+\phi_n^{\mathrm{SR}_k})}dt. \quad (6)$$

Here, $N_n^{\mathrm{SR}_k}(q)$ is a Gaussian distributed complex variable having a zero mean and a variance of N_{0k}.

Let us then S/P convert the despread symbols $\bar{d}_n^{\mathrm{SR}_k}(q)$ to generate the block-indexed vector $\boldsymbol{d}_n^{\mathrm{SR}_k}(i) = [d_n^{\mathrm{SR}_k 1}(i), \cdots, d_n^{\mathrm{SR}_k 4}(i)]^T$ with the aid of the relation $d_n^{\mathrm{SR}_k l}(i) = \bar{d}_n^{\mathrm{SR}_k}(4i+l-1)$. Furthermore, the time domain waveform of the despread symbols $d_n^{\mathrm{SR}_k l}(i)$ is given by $\hat{s}_n^{kl}(t) = \sum_{i=-\infty}^{\infty} d_n^{\mathrm{SR}_k l}(i)\psi_{T_s^{\mathrm{R}}}(t - iT_s^{\mathrm{R}})$.

Finally, the kth relay constructs the following STS-related signals $y_n^k(t)$ with the aid of the STS mapping and the spreading blocks of Fig. 1, which are given by

$$y_n^1(t) = \alpha_1\sqrt{\frac{P_{\mathrm{R}}}{4G_{\mathrm{R}}}}\sum_{q=0}^{\infty}\left\{\hat{s}_n^{11}(t)c_n^1(t-qT_s^{\mathrm{R}}) - \hat{s}_n^{12}(t)c_n^2(t-qT_s^{\mathrm{R}}) - \hat{s}_n^{13}(t)c_n^3(t-qT_s^{\mathrm{R}}) - \hat{s}_n^{14}(t)c_n^4(t-qT_s^{\mathrm{R}})\right\} \quad (7)$$

$$y_n^2(t) = \alpha_2\sqrt{\frac{P_{\mathrm{R}}}{4G_{\mathrm{R}}}}\sum_{q=0}^{\infty}\left\{\hat{s}_n^{22}(t)c_n^1(t-qT_s^{\mathrm{R}}) + \hat{s}_n^{21}(t)c_n^2(t-qT_s^{\mathrm{R}}) + \hat{s}_n^{24}(t)c_n^3(t-qT_s^{\mathrm{R}}) - \hat{s}_n^{23}(t)c_n^4(t-qT_s^{\mathrm{R}})\right\} \quad (8)$$

$$y_n^3(t) = \alpha_3\sqrt{\frac{P_{\mathrm{R}}}{4G_{\mathrm{R}}}}\sum_{q=0}^{\infty}\left\{\hat{s}_n^{33}(t)c_n^1(t-qT_s^{\mathrm{R}}) - \hat{s}_n^{34}(t)c_n^2(t-qT_s^{\mathrm{R}}) + \hat{s}_n^{31}(t)c_n^3(t-qT_s^{\mathrm{R}}) + \hat{s}_n^{32}(t)c_n^4(t-qT_s^{\mathrm{R}})\right\} \quad (9)$$

$$y_n^4(t) = \alpha_4\sqrt{\frac{P_{\mathrm{R}}}{4G_{\mathrm{R}}}}\sum_{q=0}^{\infty}\left\{\hat{s}_n^{44}(t)c_n^1(t-qT_s^{\mathrm{R}}) + \hat{s}_n^{43}(t)c_n^2(t-qT_s^{\mathrm{R}}) - \hat{s}_n^{42}(t)c_n^3(t-qT_s^{\mathrm{R}}) + \hat{s}_n^{41}(t)c_n^4(t-qT_s^{\mathrm{R}})\right\}, \quad (10)$$

with the aid of the normalization factor $\alpha_k = \sqrt{\frac{1}{P_{\mathrm{S}}\sigma_k^2 + N_{0k}}}$, where σ_k^2 represents a variance of the kth source-relay channel. As a result of the quasi-simultaneous cooperative transmission of the STS codeword of Eqs. (7)–(10), the corresponding received symbols at the destination node $r^{\mathrm{RD}}(t)$ can be expressed as

$$r^{\mathrm{RD}}(t) = \sum_{n=1}^{N}\sum_{k=1}^{4} h_n^{\mathrm{RD}_k} y_n^k(t-\tau_{nk}) e^{j(2\pi f_c t + \phi_n^{\mathrm{RD}_k})} + n_{\mathrm{RD}}(t), \quad (11)$$

where $\phi_n^{\mathrm{RD}_k} = \theta_n^{\mathrm{RD}_k} - 2\pi f_c \tau_{nk}$ and $n_{\mathrm{RD}}(t)$ has a zero mean and a variance of $N_{0\mathrm{D}}$. Note here that Eq. (11) represents the waveform superimposition of the $4N$ asynchronous relay nodes, corresponding to the N STS codewords.

III. CDSTS Detection Algorithm

At the destination node of Fig. 1, the symbols transmitted from the nth source node are detected in a low-complexity manner based both on the direct source-destination link and on the relay-destination links, so that a high diversity gain is achieved without any CSI estimation.

First, the signals received at the broadcast phase $r^{\mathrm{SD}}(t)$ in Eq. (3) are despread similarly to Eq. (4), which is expressed as

$$\bar{d}_n^{\mathrm{SD}}(q) = \sqrt{P_{\mathrm{S}}} h_n^{\mathrm{SD}} \bar{v}_n(q) + J_n^{\mathrm{SD}}(q) + N_n^{\mathrm{SD}}(q), \quad (12)$$

where we have the MUI-related component $J_n^{\mathrm{SD}}(q)$ and the AWGN-related component $N_n^{\mathrm{SD}}(q)$, such as

$$J_n^{\mathrm{SD}}(q) = \frac{1}{T_c}\sum_{n'\neq n}\sum_{q=0}^{\infty}\frac{\sqrt{P_{\mathrm{S}}}}{G_{\mathrm{S}}} h_{n'}^{\mathrm{SD}} \exp\left\{j(\phi_{n'}^{\mathrm{SD}} - \phi_n^{\mathrm{SD}})\right\} \times \int_{qT_s^{\mathrm{S}}+\tau_n}^{(q+1)T_s^{\mathrm{S}}+\tau_n} s_{n'}(t-\tau_{n'}) c_{n'}(t - qT_s^{\mathrm{S}} - \tau_{n'}) c_n(t-\tau_n) dt \quad (13)$$

$$N_n^{\mathrm{SD}}(q) = \frac{1}{T_c\sqrt{G_{\mathrm{S}}}}\int_{qT_s^{\mathrm{S}}+\tau_n}^{(q+1)T_s^{\mathrm{S}}+\tau_n} n_{\mathrm{SD}}(t) c_n(t-\tau_n) e^{-j(2\pi f_c t + \phi_n^{\mathrm{SD}})} dt. \quad (14)$$

For simplicity of the treatment, the despread symbols $\bar{d}_n^{\mathrm{SD}}(q)$ are then rearranged at the detector into the following vectorial form

$$\boldsymbol{\xi}_n^{\mathrm{SD}}(i) = \left[\ \xi_n^{\mathrm{SD}_1}(i)\ \xi_n^{\mathrm{SD}_2}(i)\ \xi_n^{\mathrm{SD}_3}(i)\ \xi_n^{\mathrm{SD}_4}(i)\ \right]^T = \frac{1}{\sqrt{4}}\begin{bmatrix} d_n^{\mathrm{SD}_1}(i) + d_n^{\mathrm{SD}_2}(i) + d_n^{\mathrm{SD}_3}(i) + d_n^{\mathrm{SD}_4}(i) \\ -d_n^{\mathrm{SD}_2}(i) + d_n^{\mathrm{SD}_1}(i) - d_n^{\mathrm{SD}_4}(i) + d_n^{\mathrm{SD}_3}(i) \\ -d_n^{\mathrm{SD}_3}(i) + d_n^{\mathrm{SD}_4}(i) + d_n^{\mathrm{SD}_1}(i) - d_n^{\mathrm{SD}_2}(i) \\ -d_n^{\mathrm{SD}_4}(i) - d_n^{\mathrm{SD}_3}(i) + d_n^{\mathrm{SD}_2}(i) + d_n^{\mathrm{SD}_1}(i) \end{bmatrix}, \quad (15)$$

with the aid of the symbol-to-block transformation $d_n^{\mathrm{SD}_l}(i) = \bar{d}_n^{\mathrm{SD}}(4i+l-1)$. Next, the signals received during the cooperative phase $r^{\mathrm{RD}}(t)$ in Eq. (11) are despread to form $\boldsymbol{\xi}_n^{\mathrm{RD}}(i) = [\xi_n^{\mathrm{RD}_1}(i)\ \xi_n^{\mathrm{RD}_2}(i)\ \xi_n^{\mathrm{RD}_3}(i)\ \xi_n^{\mathrm{RD}_4}(i)]^T$, which is given by

$$\xi_n^{\mathrm{RD}_l}(i) = \frac{1}{T_c\sqrt{G_{\mathrm{R}}}}\sum_{k=1}^{4}\int_{iT_s^{\mathrm{R}}+\tau_{nk}}^{(i+1)T_s^{\mathrm{R}}+\tau_{nk}} r^{\mathrm{RD}}(t) c_n^l(t-\tau_{nk}) e^{-j(2\pi f_c t + \phi_n^{\mathrm{RD}_k})} dt = D_n^{\mathrm{RD}_l}(i) + J_n^{\mathrm{RD}_l}(i) + N_n^{\mathrm{RD}_l}(i), \quad (16)$$

where $\boldsymbol{D}_n^{\mathrm{RD}}(i) = [D_n^{\mathrm{RD}_1}(i)\ D_n^{\mathrm{RD}_2}(i)\ D_n^{\mathrm{RD}_3}(i)\ D_n^{\mathrm{RD}_4}(i)]^T$ can be expressed as

$$\boldsymbol{D}_n^{\mathrm{RD}}(i) = \sqrt{\frac{P_{\mathrm{R}}}{4}}\times \begin{bmatrix} \frac{h_n^{\mathrm{RD}_1} d_n^{\mathrm{SR}_1}(i)}{\sqrt{P_{\mathrm{S}}\sigma_1^2+N_{01}}} + \frac{h_n^{\mathrm{RD}_2} d_n^{\mathrm{SR}_2}(i)}{\sqrt{P_{\mathrm{S}}\sigma_2^2+N_{02}}} + \frac{h_n^{\mathrm{RD}_3} d_n^{\mathrm{SR}_3}(i)}{\sqrt{P_{\mathrm{S}}\sigma_3^2+N_{03}}} + \frac{h_n^{\mathrm{RD}_4} d_n^{\mathrm{SR}_4}(i)}{\sqrt{P_{\mathrm{S}}\sigma_4^2+N_{04}}} \\ -\frac{h_n^{\mathrm{RD}_1} d_n^{\mathrm{SR}_2}(i)}{\sqrt{P_{\mathrm{S}}\sigma_1^2+N_{01}}} + \frac{h_n^{\mathrm{RD}_2} d_n^{\mathrm{SR}_1}(i)}{\sqrt{P_{\mathrm{S}}\sigma_2^2+N_{02}}} - \frac{h_n^{\mathrm{RD}_3} d_n^{\mathrm{SR}_4}(i)}{\sqrt{P_{\mathrm{S}}\sigma_3^2+N_{03}}} + \frac{h_n^{\mathrm{RD}_4} d_n^{\mathrm{SR}_3}(i)}{\sqrt{P_{\mathrm{S}}\sigma_4^2+N_{04}}} \\ -\frac{h_n^{\mathrm{RD}_1} d_n^{\mathrm{SR}_3}(i)}{\sqrt{P_{\mathrm{S}}\sigma_1^2+N_{01}}} + \frac{h_n^{\mathrm{RD}_2} d_n^{\mathrm{SR}_4}(i)}{\sqrt{P_{\mathrm{S}}\sigma_2^2+N_{02}}} + \frac{h_n^{\mathrm{RD}_3} d_n^{\mathrm{SR}_1}(i)}{\sqrt{P_{\mathrm{S}}\sigma_3^2+N_{03}}} - \frac{h_n^{\mathrm{RD}_4} d_n^{\mathrm{SR}_2}(i)}{\sqrt{P_{\mathrm{S}}\sigma_4^2+N_{04}}} \\ -\frac{h_n^{\mathrm{RD}_1} d_n^{\mathrm{SR}_4}(i)}{\sqrt{P_{\mathrm{S}}\sigma_1^2+N_{01}}} - \frac{h_n^{\mathrm{RD}_2} d_n^{\mathrm{SR}_3}(i)}{\sqrt{P_{\mathrm{S}}\sigma_2^2+N_{02}}} + \frac{h_n^{\mathrm{RD}_3} d_n^{\mathrm{SR}_2}(i)}{\sqrt{P_{\mathrm{S}}\sigma_3^2+N_{03}}} + \frac{h_n^{\mathrm{RD}_4} d_n^{\mathrm{SR}_1}(i)}{\sqrt{P_{\mathrm{S}}\sigma_4^2+N_{04}}} \end{bmatrix},$$

and the corresponding MUI component $J_n^{\mathrm{RD}}(i)$ and the noise component $N_n^{\mathrm{RD}_l}(i)$ are as follows:

$$J_n^{\mathrm{RD}}(i) = \frac{1}{T_c\sqrt{G_{\mathrm{R}}}}\sum_{k=1}^{4}\int_{iT_s^{\mathrm{R}}+\tau_{nk}}^{(i+1)T_s^{\mathrm{R}}+\tau_{nk}} c_n^l(t-\tau_{nk}) e^{-j(2\pi f_c t + \phi_n^{\mathrm{RD}_k})} \left[\sum_{n'\neq n}\sum_{k'=1}^{4} h_{n'}^{\mathrm{RD}_{k'}} y_{n'}^{k'}(t-\tau_{n'k'}) e^{j(2\pi f_c t + \phi_{n'}^{\mathrm{RD}_{k'}})} + \sum_{k'\neq k}^{4} h_n^{\mathrm{RD}_{k'}} y_n^{k'}(t-\tau_{nk'}) e^{j(2\pi f_c t + \phi_n^{\mathrm{RD}_{k'}})}\right] dt \quad (17)$$

$$N_n^{\mathrm{RD}_l}(i) = \frac{1}{T_c\sqrt{G_{\mathrm{R}}}}\sum_{k=1}^{4}\int_{iT_s^{\mathrm{R}}+\tau_{nk}}^{(i+1)T_s^{\mathrm{R}}+\tau_{nk}} n_{\mathrm{RD}}(t) c_n^l(t-\tau_{nk}) e^{-j(2\pi f_c t + \phi_n^{\mathrm{RD}_k})} dt. \quad (18)$$

According to [11], let us denote the rearranged vectorial form of the despread signals as follows:

$$\boldsymbol{\zeta}_n^{X_1}(i) = [\ \ \xi_n^{X_1}(i)\ \ \xi_n^{X_2}(i)\ \ \xi_n^{X_3}(i)\ \ \xi_n^{X_4}(i)]^T \quad (19)$$

$$\boldsymbol{\zeta}_n^{X_2}(i) = [-\xi_n^{X_2}(i)\ \ \xi_n^{X_1}(i)\ \ \xi_n^{X_4}(i) - \xi_n^{X_3}(i)]^T \quad (20)$$

$$\boldsymbol{\zeta}_n^{X_3}(i) = [-\xi_n^{X_3}(i) - \xi_n^{X_4}(i)\ \ \xi_n^{X_1}(i)\ \ \xi_n^{X_2}(i)]^T \quad (21)$$

$$\boldsymbol{\zeta}_n^{X_4}(i) = [-\xi_n^{X_4}(i)\ \ \xi_n^{X_3}(i) - \xi_n^{X_2}(i)\ \ \xi_n^{X_1}(i)]^T, \quad (22)$$

where we have X = SD or RD. Finally, based on Eqs. (19)–(22), the detector evaluates

$$\Re\left[\left\{\boldsymbol{\zeta}_n^{\mathrm{SD}_1}(i+1)\right\}^T\left\{\boldsymbol{\zeta}_n^{\mathrm{SD}_l}(i)\right\}^* + \left\{\boldsymbol{\zeta}_n^{\mathrm{RD}_1}(i+1)\right\}^T\left\{\boldsymbol{\zeta}_n^{\mathrm{RD}_l}(i)\right\}^*\right] = \left\{4P_{\mathrm{S}}\left(h_n^{\mathrm{SD}}\right)^2 + \sum_{k=1}^{4}\frac{P_{\mathrm{S}}P_{\mathrm{R}}}{P_{\mathrm{S}}\sigma_k^2+N_{0k}}\left(h_n^{\mathrm{SR}_k}h_n^{\mathrm{RD}_k}\right)^2\right\}||\boldsymbol{v}_n(i)||a_n^l(i)$$

$$+ J_n(i) + N_n(i), \tag{23}$$

where the operator $\Re[\bullet]$ indicates the real part of $\bullet$ and $J_n(i)$ represents the MUI-related term, originated from Eqs. (5), (13) and (17), while $N_n(i)$ is the AWGN-related term obeying Eqs. (6), (14) and (18). Finally, the symbols $a_n^l(i)$ are detected by the low-complexity hard decision decoder evaluating Eq. (23). It can be seen from Eq. (23) that if the multiuser interference is efficiently suppressed, our system may benefit from a maximum diversity order of five.

IV. Basic Properties of LS Codes

As represented by the term $J_n(i)$ in Eq. (23), the attainable performance of our CDSTS system is affected by the MUI, therefore dependent on the spreading codes employed. In order to mitigate the performance degradation due to the MUI, we employ LS codes [12] as the spreading codes in our CDSTS system, which exhibit a so-called IFW, where the off-peak aperiodic auto-correlation values as well as the aperiodic cross-correlation values become zero, resulting in zero ISI and zero MAI, provided that the maximum delay of the asynchronous transmissions is within the width of the IFW.

Here we only highlight the basic characteristics and the parameters of the LS codes employed, since the design of LS codes was detailed for example in [10] and in the references therein. To be specific, LS codes are constructed with the aid of a ($P_{\rm LS} \times P_{\rm LS}$)-dimensional Walsh-Hadamard matrix as well as an orthogonal complementary code set of length $N_{\rm LS}$. More specifically, by inserting W_0 zeros both at the beginning and in the center of the complementary code pair, we can generate $P_{\rm LS}$ LS codes having an IFW of $\min\{N_{\rm LS}-1, W_0\}$ chip durations, where the corresponding code length of the LS codes is $L = N_{\rm LS}P_{\rm LS} + 2W_0$. According to [10], the parameter-based notation of LS codes is given by LS($N_{\rm LS}$, $P_{\rm LS}$, W_0).

On the other hand, a particular drawback of LS codes is that they have a limited code set. For example, consider the set of LS codes LS($N_{\rm LS}$, $P_{\rm LS}$, W_0) = (4, 8, 3), having an IFW of $W_0 = 3$ chip durations and the code length of $L = N_{\rm LS}P_{\rm LS} + 2W_0 = 38$ chips. In this case the corresponding number of LS codes becomes as low as $P_{\rm LS}$ = 6, while that of the Gold codes having a similar code length of $L = 31$ chips is 33. Therefore, considering the employment of LS codes in a practical system, it is generally beneficial to combine DS-CDMA using LS codes with other multiple access schemes. For example, we may combine LS-code based CDMA with Frequency Division Multiple Access (FDMA), Time Division Multiple Access (TDMA) and Spatial Division Multiple Access (SDMA). For this reason, a hybrid TD-CDMA based channel allocation scheme is employed in our LS code-aided CDSTS system, which is reminiscent of the TDMA/CDMA philosophy of the 3G systems [12].

V. Performance and Discussion

In this section we provide performance results in order to characterize our CDSTS system, which are then followed by our discussions, including our future studies and challenges. We consider a BPSK-modulated CDSTS system supporting $N = 4$ source nodes, each of which is supported by $N_{\rm R} = 4$ source-specific relay nodes that are allocated prior to communications. The synchronization delays τ_n of the source nodes and those of the associated kth relay nodes τ_{nk} are uniformly distributed in [0, $\tau_{\max}$], where $\tau_{\max}$ is the maximum delay value, ranging from 0 to $7T_c$ in our simulations. We assumed that the source-destination and the relay-destination channels were non-dispersive Rayleigh fading channels, while the source-relay channels were either Rayleigh fading or perfect channels. We note here that the term 'perfect channel' indicates a lossless channel, leading to the ideal relaying performance in the context of the decode-and-forward scheme. As mentioned above, LS codes are employed as our DS-CDMA spreading codes, where the source nodes have the LS codes of LS($N_{\rm LS}$, $P_{\rm LS}$, W_0) = LS(8,4,7), while the relay nodes employ LS($N_{\rm LS}$, $P_{\rm LS}$, W_0) = LS(8,16,7), indicating that the corresponding width of the IFW is $7T_c$. For instance, assuming that the system has a chip rate of 1.2288 Mchips/sec, the width of the IFW becomes $7T_c$ = 5.7 μs. Furthermore, the power allocated to the souce and to the relay nodes was set to $P_{\rm S} = P_{\rm R} = 0.5$, as suggested in [6].

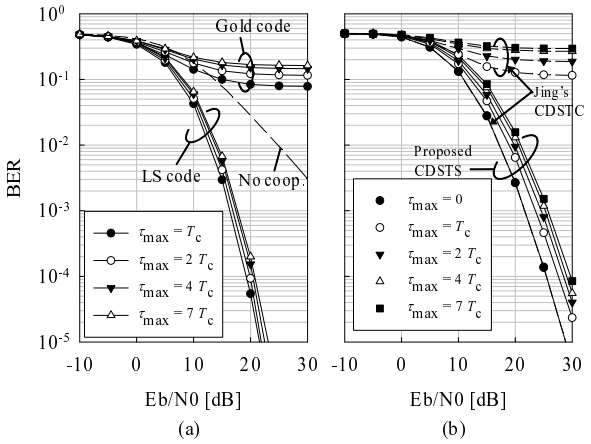

Fig. 2. Achievable BER performance of our CDSTS system in frequency-flat fading channels for the maximum delay values ranging from $\tau_{\max} = 0$ to $7T_c$, comparing (a) LS codes and Gold codes and (b) our CDSTS scheme and Jing's CDSTC scheme [6].

Fig. 2(a) shows the achievable BER performance of our CDSTS system in conjunction with the different maximum delay values of $\tau_{\max}$ = T_c, $2T_c$, $4T_c$ and $7T_c$, where the source-relay channels were assumed to be perfect. In addition to the above-mentioned LS codes, Gold codes are also considered as spreading codes in order to show the effects of diverse spreading codes on the achievable performance, noting that Gold codes constitute well-known spreading code having relatively good asynchronous cross-correlation properties [2]. Furthermore, we also characterized the non-cooperative differential transmission scenario associated with $P_{\rm S} = 1$, where the source nodes communicate with the destination node without relying on any cooperating nodes. Observe in Fig. 2(a) that regardless of the maximum delay values $\tau_{\max}$, the LS code-based CDSTS system attained a high diversity gain, outperforming the non-cooperative scenario. This implies that the MUI-induced degradations are overcome by the LS code's IFW. On the other hand, it can be seen that the performance of the Gold code-based CDSTS system is seriously deteriorated by the effects of synchronization errors. In fact, the performance became even worse than that of the non-cooperative system.

Fig. 2(b) compares our CDSTS with the CDSTC benchmarker presented by Jing and Jafarkhani [6], which employs a TDMA-based orthogonal channel allocation scheme. Therefore, unlike the TD-CDMA based channel allocation scheme of our CDSTS, Jing's CDSTC arrangement does not cause any MUI, although the relay nodes' asynchronous nature was not taken into account. We assumed in Jing's CDSTC benchmark scheme that the symbol duration was T_c and a (4×4)-element real-valued square system-matrix contained the orthogonal codes [6] employed for the STC scheme, while employing the ML detector at the destination node. Additionally, since the direct source-destination link was not considered in the benchmark system [6], the source-destination link in our CDSTS system was also ignored in order to enable a fair comparison, although this gives

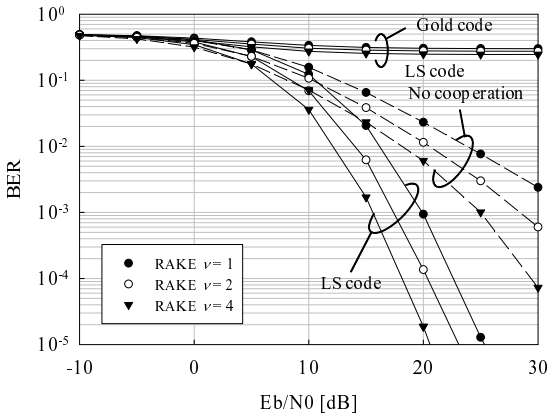

Fig. 3. Achievable BER performance of our CDSTS scheme in frequency-selective channels for different number of RAKE fingers ν = 1, 2 and 4 at the destination receiver, where we considered a correlated tapped line channel model associated with $L_{\rm tap} = 4$ taps and the tap correlation factor of ρ = 0.5. The maximum delay value was set to $\tau_{\rm max} = 3T_c$.

rise to a reduction in the resultant diversity order of our system. The source-relay channels were assumed to be Rayleigh fading channels. Observe in Fig. 2(b) that our CDSTS and Jing's CDSTC [6] schemes exhibited an identical BER performance in the case of $\tau_{\rm max} = 0$, implying that our CDSTS can indeed perfectly eliminate the effects of synchronous MUI and hence reached the BER performance of Jing's CDSTC benchmark using a TDMA-based orthogonal multiple access scheme. Furthermore, upon introducing the asynchronous relays, Jing's CDSTC exhibited an error floor due to deteriorating the orthogonality of the cooperative space-time codeword. By contrast, our LS code-based CDSTS system retained its high diversity gain in all the cases considered, although naturally the performance was degraded to some extent upon increasing the maximum delay $\tau_{\rm max}$.

Although the aforementioned systems assumed the presence of narrowband frequency-flat channels, our CDSTS system can be readily employed for transmission over broadband frequency-selective channels by introducing the concept of RAKE combining in Eq. (23). Fig. 3 shows the achievable BER performance of our CDSTS in a frequency-selective channel environment in conjunction with ν = 1, 2 and 4 RAKE fingers, where the maximum delay value was set to $\tau_{\rm max}$ = $3T_c$. Furthermore, we considered a correlated tapped delay line channel model for each channel [13], where the number of CIR taps was $L_{\rm tap} = 4$ and the correlation factor ρ_{ij} between the ith tap and the jth tap was set to $\rho_{ij} = 0.5$. For comparison, we also simulated the non-cooperative differentially-encoded transmission scheme using LS codes and the Gold code-based CDSTS benchmark scheme. In this case, the corresponding total maximum delay, namely the sum of the maximum synchronization delay $\tau_{\rm max}$ and of the tap length $L_{\rm tap}$, becomes $7T_c$, which is within the IFW. The source-relay channels were assumed to be perfect. It is seen in Fig. 3 that both our LS code-based CDSTS arrangement and the non-cooperative scenario using LS codes benefitted from an increased path diversity gain upon increasing the number of RAKE fingers ν owing to the ideal auto-correlation characteristics of the LS codes. More specifically, our LS code-based CDSTS is capable of gleaning both space-time diversity gain as well as path diversity gain and hence outperformed both the non-cooperative scenario as well as the Gold code-based CDSTS benchmark scheme.

Our CDSTS system was designed so that the total maximum asynchronous delay becomes less than the IFW width of LS codes for the sake of circumventing the asynchronous nature of the relay nodes. However, the number of LS codes exhibiting a sufficiently wide IFW is limited. Hence LS codes strike a design tradeoff between the code length $L_{\rm LS}$, the number of codes $P_{\rm LS}$ and the IFW width W_0. To extend the degree of design freedom and hence accommodate large synchronous delays, Multi-Carrier (MC) transmission can be incorporated into our CDSTS system, as described in [10]. More specifically, the IFW duration of the LS codes can be extended by a factor of the number of subcarriers, since the chip duration of each subcarrier is proportionately increased.

VI. Conclusion

In this contribution we proposed a practical cooperative differential space-time diversity protocol, where neither channel estimation nor symbol-level synchronization is required at the nodes. More specifically, cooperative space-time diversity is achieved with the aid of our LS code-based STS scheme relying on cooperating asynchronous nodes. Our simulation results demonstrate that unlike the previously-proposed CDSTC of [6], the proposed CDSTS scheme is capable of combating the effects of asynchronous transmissions, provided that the maximum synchronization delay of the relay nodes is within the width of the IFW. Furthermore, our CDSTS scheme is capable of gleaning path diversity gain in addition to space-time diversity gain with the aid of RAKE combining at the destination receiver.

References

[1] B. Hochwald, T. Marzetta, and C. Papadias, "A transmitter diversity scheme for wideband CDMA systems based on space-time spreading," *IEEE Journal on Selected Areas in Communications*, vol. 19, no. 1, pp. 48–60, 2001.

[2] L. Hanzo, L.-L. Yang, E.-L. Kuan, and K. Yen, *Single and Multi-Carrier CDMA: Multi-User Detection, Space-Time Spreading, Synchronisation and Standards*. John Wiley and IEEE Press, 2003, **1060 pages**.

[3] J. Laneman and G. Wornell, "Distributed space-time-coded protocols for exploiting cooperative diversity in wireless networks," *IEEE Transactions on Information Theory*, vol. 49, no. 10, pp. 2415–2425, 2003.

[4] Y. Jing and B. Hassibi, "Distributed space-time coding in wireless relay networks," *IEEE Transactions on Wireless Communications*, vol. 5, no. 12, p. 3524, 2006.

[5] B. Hochwald and W. Sweldens, "Differential unitary space-time modulation," *IEEE Transactions on Communications*, vol. 48, no. 12, pp. 2041–2052, 2000.

[6] Y. Jing and H. Jafarkhani, "Distributed differential space-time coding for wireless relay networks," *IEEE Transactions on Communications*, vol. 56, no. 7, pp. 1092–1100, 2008.

[7] R. C. Palat, A. Annamalai, and J. H. Reed, "Accurate bit-error-rate analysis of bandlimited cooperative OSTBC networks under timing synchronization errors," *IEEE Transactions on Vehicular Technology*, vol. 58, no. 5, pp. 2191–2200, 2009.

[8] Y. Li and X. Xia, "A family of distributed space-time trellis codes with asynchronous cooperative diversity," *IEEE Transactions on Communications*, vol. 55, no. 4, pp. 790–800, 2007.

[9] Z. Li and X. Xia, "An Alamouti coded OFDM transmission for cooperative systems robust to both timing errors and frequency offsets," *IEEE Transactions on Wireless Communications*, vol. 7, no. 5 Part 2, pp. 1839–1844, 2008.

[10] H. Wei, L.-L. Yang, and L. Hanzo, "Interference-free broadband single-and multicarrier DS-CDMA," *IEEE Communications Magazines*, vol. 43, no. 2, pp. 68–73, 2005.

[11] M. El-Hajjar, O. Alamri, S. X. Ng, and L. Hanzo, "Turbo detection of precoded sphere packing modulation using four transmit antennas for differential space-time spreading," *IEEE Transactions on Wireless Communications*, vol. 7, no. 3, pp. 943–952, 2008.

[12] L. Hanzo, J. Blogh, and S. Ni, *3G, HSPA and FDD versus TDD Networking: Smart Antennas and Adaptive Modulation*. John Wiley and IEEE Press, 2008, **564 pages**.

[13] J. Wu, C. Xiao, and K. Letaief, "Multiuser channel estimation for CDMA systems over frequency-selective fading channels," *IEEE Transactions on Wireless Communications*, vol. 4, no. 4, pp. 1724–1736, July 2005.